Observation of noisy precursors of dynamical instabilities

Carson Jeffries
Physics Department, University of California, Berkeley, California 94720
and Materials and Molecular Research Division, Lawrence Berkeley Laboratory, Berkeley, California 94720

Kurt Wiesenfeld
Physics Department, University of California, Berkeley, California 94720
(Received 2 July 1984)

We have measured the power spectra of a periodically driven p-n junction in the vicinity of a dynamical instability. The addition of external noise introduces new lines in the spectra, which become more prominent as a bifurcation point is approached. The scaling of the peak, width, area, and line shape of these lines is measured near the onset of two different codimension-one instabilities: the period doubling and Hopf bifurcations. The results are in excellent agreement with recent theoretical predictions.

I. INTRODUCTION

Nonlinear dynamical systems displaying a variety of complex behavior have been the subject of much research over the last decade. Of obvious physical relevance is the effect of external random noise on these systems. For example, several investigators have studied the effect of noise on the scaling behavior of an infinite sequence of period doublings, which in the absence of noise leads to deterministic chaos.[1–6]

More recently,[7] a theory was developed to predict the effect of random noise on the power spectra of systems displaying stable periodic behavior as those systems *approach* a dynamical instability. It was found that noise induces new features in the power spectra, and that these "noisy precursors" become more prominent as the instability is approached. Here, we report results of experiments designed to test the predictions of that theory.

The most striking result of the theory is that the details of the dynamical system are unimportant for the main features of the power spectrum. Instead, there are only a small number of qualitatively distinct precursors; the one observed in any specific situation depends on the class of instability the system is near. The classification, furthermore, follows solely from the *deterministic* dynamical system.

The notion that seemingly unrelated physical systems behave the same quantitatively in the vicinity of an instability is most familiar from the study of critical phenomena in statistical mechanics. The great success of the renormalization group leads to the grouping together of varied systems undergoing phase transitions into universality classes. In an analogous way, bifurcation theory[8] allows one to classify the behavior of nonlinear dynamical systems in the vicinity of a dynamical instability, or bifurcation. Reference 7 showed that this classification scheme could be extended to include the effect of random noise near an instability for systems displaying time-periodic behavior. In particular, quantitative results were derived for the *codimension-one bifurcations,* i.e., instabilities encountered as a single control parameter is varied. A similar extension for the codimension-one bifurcations of time-independent behavior was previously derived within the framework of a Fokker-Planck analysis.[9]

The same set of noisy precursors should therefore appear in all types of dynamical systems. The experiments described in the following were performed on a well-characterized nonlinear physical system, a driven p-n junction;[13,17,22] similar results should be seen, for example, in laser systems[10] and hydrodynamical systems.[11]

Section II reviews the basic ideas and predictions of the theory. Section III describes the physical system and procedures used in the experiments. Sections IV and V present the results for the period doubling and Hopf bifurcations, respectively. Finally, a brief discussion is presented in Sec. VI.

II. THEORY

In this section, we summarize the theory of noisy precursors. A complete mathematical analysis is presented in Ref. 7; here, we emphasize the physical picture behind the theory, and state the main results.

The aim is to analyze the power spectrum of a periodic system subject to external noise, when the system is near a dynamical instability. Suppose that the dynamics is governed by the set of differential equations

$$\dot{\underline{x}}=\underline{F}(\underline{x},t;\lambda),\quad \underline{x}\in\mathbb{R}^n\,, \tag{1}$$

where $\underline{F}$ depends on some adjustable parameter λ, and that the system has an asymptotically stable T-periodic solution $\underline{x}_0(t)$:

$$\underline{x}_0(t+T)=\underline{x}_0(t)\,. \tag{2}$$

In the absence of noise, the observed power spectrum is a sequence of δ functions at frequencies $\omega=0$, $2\pi/T$, $4\pi/T$, $6\pi/T$, etc. We want to see how the power spectrum changes when external noise is added.

In phase space, $\underline{x}_0(t)$ sweeps out a closed orbit. An external perturbation can kick the system off of this orbit.

After a single small kick, the subsequent evolution is governed by Eq. (1) linearized about $\underline{x}_0$

$$\dot{\underline{\eta}}=\underline{D}(\underline{x}_0;\lambda)\underline{\eta}\ , \tag{3}$$

where $\underline{\eta}\equiv\underline{x}-\underline{x}_0$ is the deviation from the periodic orbit, and $\underline{D}$ is the matrix of partial derivatives

$$D_{ij}\equiv\left.\frac{\partial F_i}{\partial x_j}\right|_{\underline{x}=\underline{x}_0}\ . \tag{4}$$

The effect of external noise is to continuously kick the system, and may be modeled by adding a random function of time to Eq. (3)

$$\dot{\underline{\eta}}=\underline{D}(\underline{x}_0;\lambda)\underline{\eta}+\underline{\xi}(t)\ , \tag{5}$$

where $\underline{\xi}$ is a Gaussian white noise

$$\langle\underline{\xi}(t)\rangle=0,\quad\langle\xi_i(t)\xi_j(t')\rangle =\kappa_{ij}\delta(t-t')\ . \tag{6}$$

The results obtained in Ref. 7 were derived explicitly for delta-correlated noise, but are valid for more realistic noises provided that the correlation time of the second moment is short compared with all time scales relevant to the deterministic system.

Equation (5) is a linear, inhomogeneous equation with periodic coefficients, and may be solved by employing the results of the Floquet theory.[12] Of particular significance are the Floquet multipliers μ_j, which arise from special solutions $\underline{\chi}_j$ of the homogeneous equation (3), such that

$$\underline{\chi}_j(t+T)=\mu_j\underline{\chi}_j(t)\ . \tag{7}$$

The $\underline{\chi}_j$ may be thought of as transient responses of the system to an external impulse. Since $\underline{x}_0$ is asymptotically stable, the $\underline{\chi}_j$ diminish with time, so the (possibly complex) Floquet multipliers must all lie inside the unit circle

$$|\mu_j|<1\ \text{ for all } j\ . \tag{8}$$

As the single parameter λ is varied [see Eq. (5)], the μ_j move around in the complex plane—an instability is signaled when one or more of the μ_j exit the unit circle. According to the results of bifurcation theory,[8] the periodic orbit $\underline{x}_0$ will generically lose stability in one of three ways:

(i) a single multiplier $\tilde{\mu}$ may exit the unit circle along the positive real axis;

(ii) a single multiplier $\tilde{\mu}$ may exit the unit circle along the negative real axis;

(iii) a pair of complex conjugate multipliers $(\tilde{\mu},\tilde{\mu}^*)$ exit the unit circle, off the real axis.

From Eq. (7), we see that close to the instability the transient response is dominated by a single $\underline{\chi}_j$ in cases (i) and (ii), and by a pair of $\underline{\chi}_j$ in case (iii). Furthermore, the transient recovery or "relaxation" time τ is governed solely by the near-critical multiplier $\tilde{\mu}$. This last fact may be exploited to experimentally measure $\tilde{\mu}$—we return to this point in the following. The long-lived transient response to perturbations is responsible for new features in the observed power spectrum.

The dominance of the near-critical multiplier(s) simplifies the analysis of the full Eq. (5) tremendously, and is the origin of the fact that *the main features of the noisy precursors in the power spectrum depend only on the class of instability approached, and not on the details of the dynamical equation (1).* In fact, case (i) already noted may be subdivided into two distinct classes, depending on the existence or absence of a symmetry in the system.[7]

We return to the relation between $\tilde{\mu}$ and the relaxation time τ of the noiseless system subject to a single impulse. Equation (7) may be rewritten as

$$\underline{\chi}_j(t)=e^{\rho_j t}\underline{P}_j(t)\ , \tag{9}$$

where $\underline{P}_j(t)$ is a T-periodic function, and the Floquet exponents ρ_j are related to the corresponding Floquet multipliers μ_j via

$$\mu_j=e^{\rho_j T}\ . \tag{10}$$

The stability condition (8) may be expressed as

$$\mathrm{Re}\rho_j<0\ \text{ for all } j\ . \tag{11}$$

The near-critical multiplier $\tilde{\mu}$ corresponds to the exponent $\tilde{\rho}$ with the smallest (negative) real part, and from Eq. (9) we see that the relaxation time is given by

$$\tau=(-\mathrm{Re}\tilde{\rho})^{-1}\equiv\epsilon^{-1}\ . \tag{12}$$

The small quantity ϵ is a natural bifurcation parameter—it is zero at the onset of the instability. The detailed calculations of Ref. 7 show that ϵ determines the size and shape of precursor lines represent in the power spectrum, while $\mathrm{Im}\tilde{\rho}$ determines the position of the precursor lines. Quite generally, the precursor lines are centered at frequencies $\omega=2\pi n/T\pm\mathrm{Im}\tilde{\rho}$, $n=0,1,2,\ldots$, while the line shape is given by

$$S(\omega)\sim\frac{\kappa}{\epsilon^2}\left[1+\left[\frac{\omega-\omega_0}{\epsilon}\right]^2\right]^{-1}\ , \tag{13}$$

where κ is the intensity of the external noise as defined in Eq. (6), i.e., κ is the added external noise power. The scaling of these Lorentzian lines is shown in Fig. 1.

The general nature of the scaling is easy to understand. As $\epsilon\to0$, the transient response is more lightly damped, which has two effects: first, the power contained in the precursor line grows proportionally to $\tau=1/\epsilon$, and second, the line becomes narrower, the width being proportional to ϵ. The power in the precursor also grows with increasing noise power κ. Together, these imply that the peak of the Lorentzian must grow as $\kappa\epsilon^{-2}$.

In the present experiments, we were able to test these predictions for cases (ii) and (iii) already noted, called the period doubling and Hopf bifurcations, respectively. Since the intrinsic noise level of our system is very low, we could make direct measurements of the parameter ϵ by

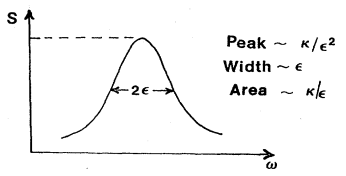

FIG. 1. Scaling of the noisy precursor lines, as given by Eq. (13).

using Eq. (12): The noiseless system is given a single, short perturbing pulse, and the damped oscillations of the transient response is then measured for its decay time τ (see Sec. III).

III. PHYSICAL SYSTEM AND EXPERIMENTAL PROCEDURES

We performed experiments to observe noisy precursors for period doubling bifurcations on a simple physical system—a resonantly driven silicon p-n junction, shown in Fig. 2. This system has been studied in detail[13–23] and is well characterized. It is essentially a driven nonlinear asymmetric oscillator. Recall the nonlinear charge storage properties of a p-n junction:[24] electrons from the n region diffuse into the p region (Fig. 2), annihilating with holes and leaving a net charged layer of donor and acceptor ions fixed in the lattice, together with a built-in potential difference Φ. For an applied reverse bias voltage V, solution of the partial differential equations of diffusion and drift yields a junction differential capacitance

$$C_j=\frac{\partial Q}{\partial V}=C_{j0}(1+V/\Phi)^{-\beta} ,$$

where $\beta\approx 0.5$, typically. For a forward bias voltage, holes (electrons) are injected into the n (p) region, where they become minority carriers, recombinating with electrons (holes) and also diffusing back in a characteristic lifetime τ_1. However, for times $t\lesssim\tau_1$ following injection, this can result in a rather large charge storage capacitance

$$C_S=C_{S0}\exp(V/\varphi) ,$$

where $\varphi=kT/e$. The junction also conducts according to the Shockley relation

$$I_d(V)=I_0[\exp(V/\varphi)-1]$$

for the junction current.

Our experimental arrangement (Fig. 2) shows a p-n junction of assumed total differential capacitance $C_d(V)=C_j+C_s$, in series with an inductance L and resistance R, driven by a summing amplifier $\sum$, with output driving point voltage

$$V_0(t)=V_S(t)+V_N(t)+V_P(t) . \tag{14}$$

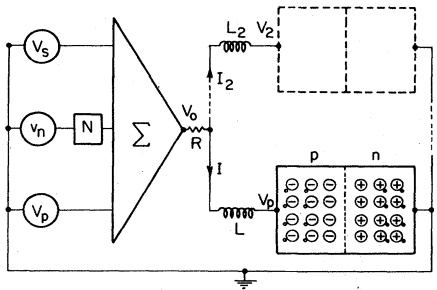

FIG. 2. Experimental arrangement: a p-n junction driven resonantly through an inductance L and resistance R by a voltage V_0, which is the linear sum of voltages V_S, V_P, and v_n (reduced by attenuator N). A single p-n junction is used for period doubling bifurcations; a second (upper) identical is added to observe a Hopf bifurcation. The junction is a Si crystal containing + donor ions and electrons (·) in the n region, and − acceptor ions and holes (○) in the p region.

Here, $V_0(t)=V_{0S}\cos(\omega_0 t)$ is a driving sinusoid of precisely controllable amplitude V_{0S} and frequency ω_0, chosen to be approximately

$$\omega_{\rm res}=[LC_d(V_{0S}=0)]^{-1/2} ,$$

i.e., at the resonant frequency of the inductor-junction resonator at very low driving voltage. The voltage $v_n(t)$ is a wide-band white random noise voltage generated from the amplified current of a Zener (avalanche breakdown) diode. Together with a precision attenuator N of range 0 to −100 dB, this provides a variable noise voltage $V_N(t)$ at the driving point. The voltage $V_P(t)$ is a perturbing pulse used for measuring the recovery time τ_c (i.e., the critical slowing down time) of the system near a bifurcation point and hence to provide a direct measure of relative values of the parameter $\epsilon=\tau^{-1}\approx\tau_c^{-1}$ introduced in Sec. II.

By solving the equations of motion of the system, it can be shown to be equivalent to a driven damped oscillator with a very nonlinear asymmetric restoring force.[18,22] With $V_N=0$, $V_P=0$, the system can be driven at increasing values of V_{0S} and displays a cascade of period doubling bifurcations leading to chaos, as shown in the bifurcation diagram of Fig. 3, obtained by sampling and plot-

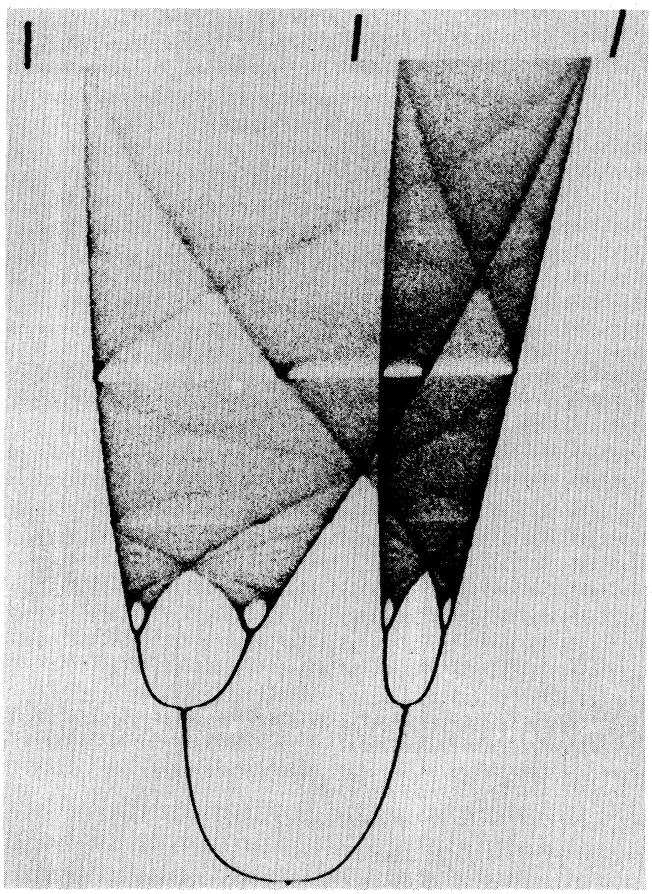

FIG. 3. Typical bifurcation diagram for driven p-n junction (Fig. 2), showing a period doubling cascade, chaos, and periodic windows. Plotted is the set of consecutive current maxima $\{I_n\}$ (horizontal) versus amplitude of sinusoidal drive voltage V_{0S} (vertical).

ting consecutive junction current maxima $\{I_n\}$. Corresponding power spectra [Fig. 4(a)] show peaks at $f_0, f_0/2, f_0/4, \ldots$, and their harmonics. A two-parameter study has been made[22] with V_{0S} and ω_0 as control parameters, yielding the phase diagram Fig. 5, with these features: characteristic hysteresis jump phenomenon of a driven nonlinear oscillator,[25] period doubling, onset of chaos, band merging (e.g., $2\rightarrow 1$), periodic windows (e.g., 3,6), crises, and hysteresis.

The effect of added random noise has been previously studied experimentally for this system,[6] with a value of the noise sensitivity scaling factor $\Gamma = 6.4 \pm 0.2$ found to be consistent with the theoretical prediction $\Gamma = 6.649\ldots$ of Crutchfield, Nauenberg, and Rudnick.[2] The scaling factor Γ is defined as follows: for added noise voltage V_N^*, suppose the cascade of period doubling bifurcations is terminated (i.e., obscured) at some period T. Then if the added noise is increased to ΓV_N^*, the cascade will be terminated at period $T/2$.

In summary, the driven p-n junction has been abundantly studied and is perhaps the best candidate for quantitative testing of the predictions of Sec. II for the period doubling instability of a periodic system.

By the addition of a second identical p-n junction resonator, shown by dashed upper lines in Fig. 2, we achieve a simple system that displays a Hopf bifurcation to quasiperiodicity.[22] The phase diagram for two coupled junctions is shown in Fig. 6, and power spectra in Figs. 4(b) and (c). At driving frequency $f_0 = 27$ kHz, there is first a period doubling bifurcation ($1\rightarrow 2$) at $V_{0S} = 0.6\,V_{\rm rms}$, and then a Hopf bifurcation at $V_{0S} = 3\,V_{\rm rms}$ to a new incommensurate frequency $f_1 \approx (0.23) f_0$. The power spectrum [Fig. 4(c)] shows peaks at the combination frequencies $f_{nm} = nf_0/2 + mf_1$, where n and m are integers. The Poincaré section is that of a 2-torus. We use this system to study noisy precursors near a Hopf bifurcation.

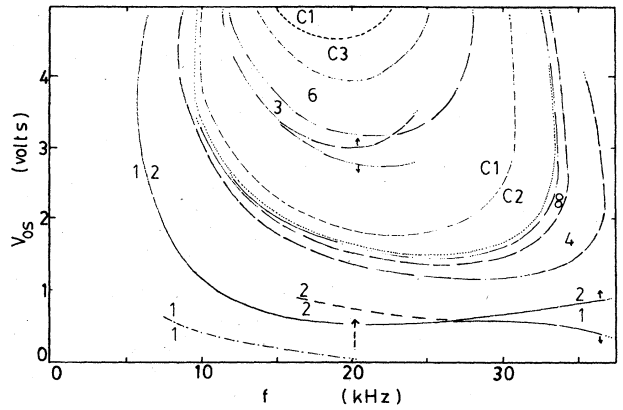

FIG. 5. Phase diagram V_{0S} versus f for single p-n junction [Ref. (22)]. The noise-induced precursor is studied along the dotted arrow.

In the experiments we measure the frequency spectrum of the junction voltage $V_d(t)$ using a Hewlett-Packard 3580A scanning spectrum analyzer with scan range $0 < f < 50$ kHz, maximum sensitivity 30 nV Hz$^{-1/2}$, and spurious frequency rejection 80 dB. It has two output modes: linear voltage $V(f) = \{\langle [V_d(t)]^2 \rangle\}^{1/2}$; and log power $10 \log_{10} P(f) = 10 \log_{10} \langle V_d^2(t) \rangle$ in dB, where the average is taken over a selected bandwidth Δf; typically $\Delta f < 10$ Hz $\ll$ line width of noisy precursor. Both linear and log power spectra were recorded for various values of

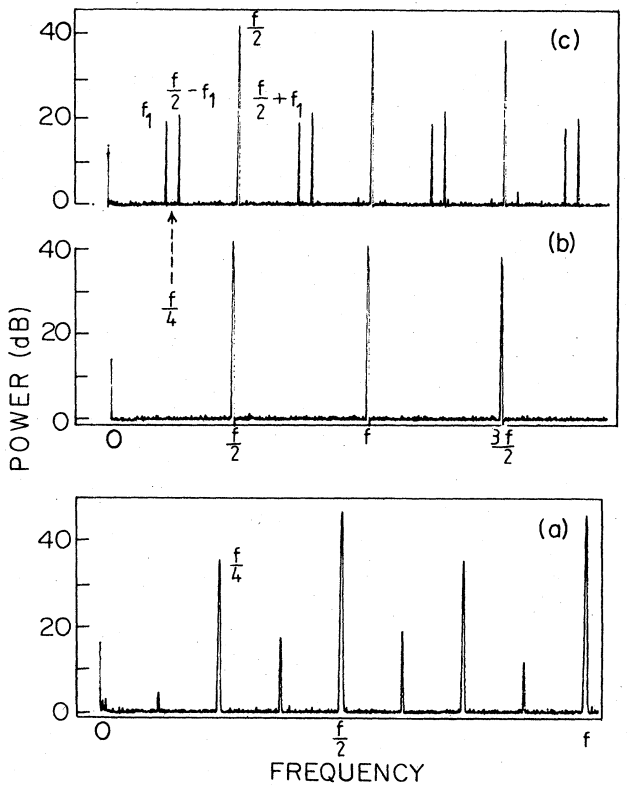

FIG. 4. Power spectra: $10 \log_{10} P(f)$ (in dB) versus frequency f. (a) For single p-n junction, showing period doubling up to period 8, $f = f_0 = 20$ kHz. (b) For two coupled p-n junctions at a drive voltage $V_{0S} = 3.20\,V_{\rm rms}$, after period doubling, $f = f_0 = 27$ kHz. (c) At $V_{0S} = 3.35\ V_{\rm rms}$, after a Hopf bifurcation to a second frequency $f_1 < f_0/4$.

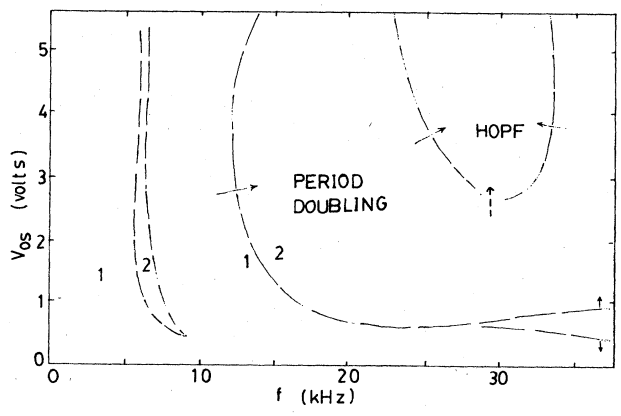

FIG. 6. Phase diagram for two coupled p-n junctions [Ref. (22)] showing the domain of $1\rightarrow 2$ period doubling and Hopf bifurcations. The noise-induced precursor is studied along the dotted arrow.

additive noise voltage $V_N = 1.2\ mV_{\rm rms} \times 10^{N/20} \times \sqrt{B}$. Here B is the band width of the summing or driving amplifier ($\sim 10^5$ Hz, typically) and N (in dB) is the noise attenuator setting (Fig. 2). We refer to N as the added noise (in dB). Data were taken for various values of $\Delta V \equiv V_{\rm th} - V_{0S}$, the deviation of the driving voltage from its bifurcation threshold value $V_{\rm th}$. To directly relate ΔV to the theoretical parameter ϵ introduced in Eq. (12), we apply a short perturbing pulse $V_P(t)$ and record the transient $V_d(t)$ on an oscilloscope to measure the time τ_c for the damped orbit to decay to $\frac{1}{3}$ of its initial value; this time is expressed as the number of cycles N_c of the period f_0^{-1}. For the period doubling case the experimental result is N_c (cycles) $\approx (\Delta V V_{\rm rms} 10^{-3})^{-1\pm 0.01}$. We assume that data for a measured value of N_c correspond directly to the model with $\epsilon \propto \tau_c^{-1} \propto N_c^{-1}$. For a Hopf bifurcation we similarly measure the decay time of the damped orbit, finding $N_c \propto (\Delta V)^{-0.8}$.

To summarize, we rewrite the theoretical power spectrum prediction [Eq. (13)] $S(\omega,\kappa,\epsilon)$ in terms of *measured quantities*

$$P(\nu,N,N_c) \propto N N_c^2 [1+(\nu/\nu_0)^2]^{-1} \quad (15)$$

for a Lorentzian line centered at relative frequency $\nu=0$, with half-width at half maximum equal to $\nu_0 \propto N_c^{-1}$. We assume the correspondences $\kappa \rightarrow N$ and $\epsilon \rightarrow N_c^{-1}$. We further assume that the linear spectrum $V(\nu,N,N_c)$ to be given by the square root of Eq. (15).

IV. EXPERIMENTAL RESULTS: PERIOD DOUBLING BIFURCATION

Figure 7 shows power spectra for a junction driven at $f_0 = 20$ kHz, slightly below the threshold for $1 \rightarrow 2$ doubling, for which $N_c \approx 27$ cycles. The precursor peaks at $f_0/2$, $3f_0/2$, and $5f_0/2$ are shown for noise attenuation settings $N = -100$, -50, and -30 dB, respectively, for Figs. 7(a)–(c). For Fig. 7(a) the residual stochastic noise of the junction system itself exceeds that added ($N = -100$ dB) and is equivalent to $N_{\rm eq} \approx -60$ dB. Figure 8 is a linear voltage frequency spectrum, $V(f)$ versus f for $N = -50$ dB, on an expanded frequency scale of the precursor at $3f_0/2 = 30$ kHz. Data are shown for three different values of ΔV, corresponding to $N_c = 10$, 26, and 55, respectively for Figs. 8(a)–(c). This clearly displays the decrease in width and increase in height of the line as N_c is increased toward the bifurcation point. The points (+) are computed from the expression for a Lorentzian line,

$$V(\nu) = H[1+8(\nu/\nu_3)^2]^{-1/2}, \quad (16)$$

where H is the observed peak height, $V(\nu=0)=H$, and ν_3 is the observed line half-width at one third of H. Except for a small asymmetry in the observed line shape, the fit is quite good and verifies the prediction of Sec. II.

Figure 9 is a plot of the precursor peak power $P(\nu=0)$ versus the added noise power N for several values of N_c. For the linear region -70 dB $< N < -20$ dB we find, independently of N_c,

$$P(\nu=0) \propto N^{1.0\pm 0.05} \quad (17)$$

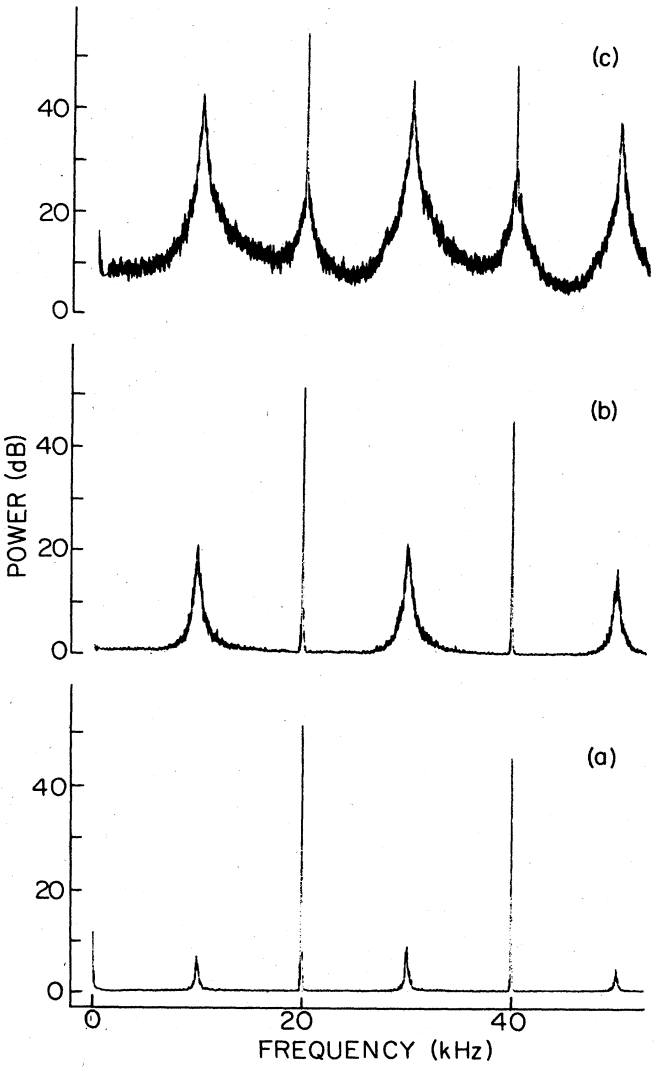

FIG. 7. Power spectra in dB for precursors at $f_0/2$, $3f_0/2$, and $5f_0/2$ with $f_0 = 20$ kHz and V_{0S} set at $\Delta V \approx 0.015\,V$ before the $1 \rightarrow 2$ period doubling threshold. (a) Noise attenuation $N = -100$ dB; (b) $N = -50$ dB; (c) $N = -30$ dB.

The upturn of the data at high attenuator setting, $N < -60$ dB, is due to the intrinsic residual noise $N_{\rm eq}$ in the system before V_N is added. (Recall that N is the attenuation of the controlled added noise.) The precursor is induced by the total noise $N_{\rm eq} + N$. The departure from linearity for small attenuation, $N > -20$ dB, is not fully understood. However, we measured the quantity $\langle V_d^2 \rangle$ in dB at $f_0 \approx f_{\rm res}$ with $V_{0S} = 0$ and found a linear dependence on N (in dB) up to $N > -20$ dB, where $\langle V_d^2 \rangle$ saturated and then decreased at $N \sim 0$ dB due to nonlinear noise-induced frequency shifting of the system resonance to below f_0 at this high noise level. We note, nevertheless, that the saturation effect in Fig. 9, and also in Fig. 12 for the Hopf bifurcation, may be due to departure from the simple theoretical model of Sec. II. Indeed, the simple scaling is *expected* to break down very close to the bifur-

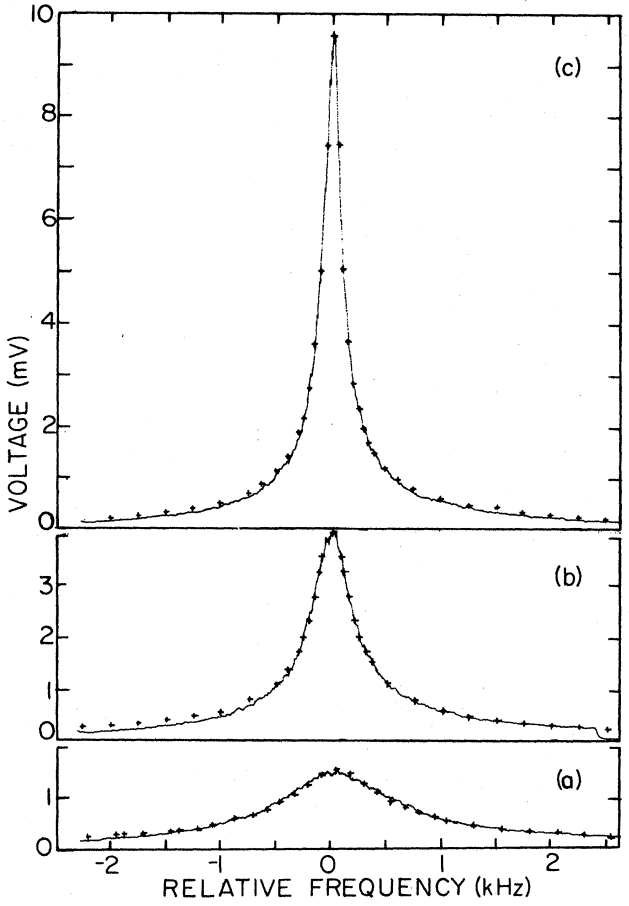

FIG. 8. Voltage frequency spectrum, $V_d(\nu)$ versus ν expanded about the line at $3f_0/2$ of Fig. 7, for added noise $N=-50$ dB, showing observed precursor line shape (solid line) and computed (crosses) Lorentzian shapes [Eq. (16)]. (a) $\Delta V=0.0403\,V_{\rm rms}$, $N_c=10$; (b) $\Delta V=0.0155\,V_{\rm rms}$, $N_c=20$; (c) $\Delta V=0.006\,V_{\rm rms}$, $N_c=55$.

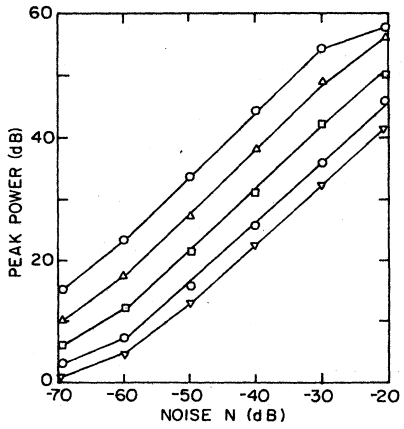

FIG. 9. Precursor peak power $P(\nu=0)$ versus added noise power N for several values of V_{0S} below the threshold for $1\rightarrow 2$ period doubling, $\Delta V=0.01$ to $0.1\,V_{\rm rms}$. The average slope of the linear region is $1.0\pm.05$.

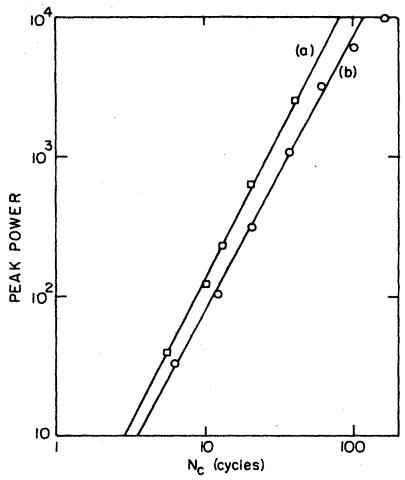

FIG. 10. Relative precursor peak power $P(\nu=0)$ versus lifetime N_c of transient orbits; (a) below threshold for period doubling, $N=-40$ dB, slope$=2.05\pm0.1$; (b) below threshold for Hopf bifurcation, $N=-50$ dB, slope$=1.97\pm0.1$.

cation point, at a parameter value dependent on the added noise intensity.[7]

To measure the dependence of precursor peak power on N_c, we took data for constant additive noise and variable N_c, with the results shown in Fig. 10(a), yielding

$$P(\nu=0)\propto N_c^{2.05\pm0.1}\,. \tag{18}$$

For a series of frequency spectra similar to Fig. 8, we measured the precursor peak voltage height H and the half-width at half maximum w and plot each versus N_c in Fig. 11 with the results

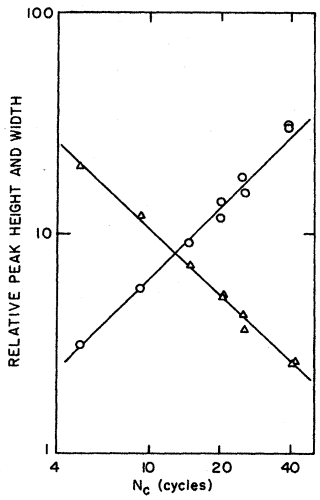

FIG. 11. Relative peak height H (0) and half-width $w(\Delta)$ of precursor line shape $V_d(f)$ (cf. Fig. 8), as a function of damping time N_c.

$$H \propto \sqrt{P(\nu=0)} \propto N_c^{1.03\pm0.05} , \tag{19}$$

$$w \propto \nu_0 \propto N_c^{-1.02\pm0.05} . \tag{20}$$

For these data we also compute and plot the product $H^2 w$ versus N_c, finding a line of slope 1.12 ± 0.1, the uncertainty due to scatter of data points. We interpret these results as an experimental indication that the area

$$A = \int P(f) df \propto N_c^{1.12} \propto \epsilon^{-1.12\pm0.1} , \tag{21}$$

which should be compared with Fig. 1, $A \propto \epsilon^{-1}$.

To summarize, all the results [Eqs. (17)—(21)] are consistent with the predictions [Eq. (16)].

V. EXPERIMENTAL RESULTS: HOPF BIFURCATION

For the system with two coupled junctions (Fig. 2) with phase diagram (Fig. 6) and power spectrum [Fig. 4(c)], we have measured the effect of added noise on the peak of the precursor of the second frequency f_1 for a set of values of ΔV below the Hopf bifurcation threshold. These data (Fig. 12) show that over the range -60 dB $< N < -40$ there is a simple relationship

$$P(\nu=0) \propto N^{0.88\pm0.1} . \tag{22}$$

Deviation from straight line behavior for large and small N are undoubtedly due to the same reasons discussed in the last section: residual noise and nonlinear resonance shifts. Other data near a Hopf bifurcation give an exponent $\sim 1.0\pm0.1$ in Eq. (22).

In Fig. 10(b) we show measured values of the peak power height for the precursor as a function of measured values of the decay time N_c. The results are

$$P(\nu=0) \propto N_c^{1.97\pm0.05} . \tag{23}$$

From a linear spectrum scan we have measured the peak precursor voltage $H = P(\nu=0)$ and the width w, shown in Fig. 13 for $N = -40$ dB,

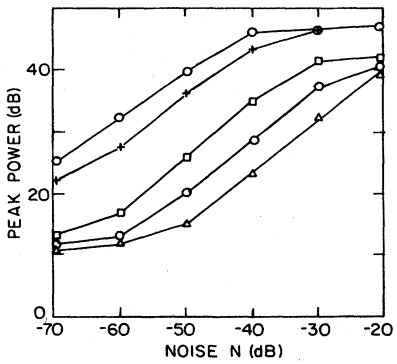

FIG. 12. Precursor peak power $P(\nu=0)$ (in dB) versus added noise N in dB for several values of V_{0S} below the Hopf bifurcation threshold, $\Delta V = 0.01$ to $0.61\, V_{\rm rms}$. The average straight line slope is 0.88 ± 0.1.

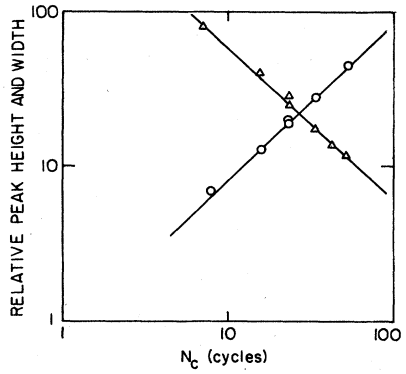

FIG. 13. Relative peak height H (0) and half-width (Δ) for precursor line shape $V_d(f)$ for Hopf bifurcation at $N = -40$ dB, $f_1 = 6.744$ kHz, and $f_0 = 20$ kHz.

$$H \propto N_c^{1.03\pm.05} , \tag{24}$$

$$w \propto N_c^{-0.99\pm.05} . \tag{25}$$

The measured quantity $H^2 w$ versus N_c has a slope 1.09 ± 0.1 implying that

$$A = \int P(f) df \propto \epsilon^{-1.09\pm0.1} . \tag{26}$$

In summary, the results [Eqs. (22)—(26)] are consistent with theoretical expectations [Eq. (15)].

VI. DISCUSSION

We have seen that the predictions of Ref. 7, as summarized in Fig. 1, correctly describe the noise induced features observed in these experiments. The scaling of the height and width with bifurcation parameter ϵ were separately tested, since the experiment provided a means for *independently* determining ϵ via measurement of the relaxation time τ in the absence of noise. Carefully measured precursor lineshapes were found to be Lorentzian, again in agreement with the theory.

We close by making a qualitative observation. In Fig. 7, the broad precursor lines appear only at the *odd harmonics* of the half-fundamental, while the lines due to the basic oscillation remain narrow. This is the signature of a nonautonomous dynamical system—that is, a system whose evolution equation (1) depends explicitly on time, which is the case for the experiments reported here. On the other hand, the theory of noisy precursors predicts that for autonomous systems, broadening of the fundamental frequency line will occur in addition to the precursor features observed in driven systems.[7]

ACKNOWLEDGMENTS

One of us (C.D.J.) thanks the Miller Institute for Basic Research in Science for support. This work was supported by the Director, Office of Energy Research, Office of Basic Energy Sciences, Materials Sciences Division of the U.S. Department of Energy under Contract No. DE-AC03-76SF00098.

[1]J. P. Crutchfield and B. A. Huberman, Phys. Lett. **77A**, 407 (1980).
[2]J. P. Crutchfield, M. Nauenberg, and J. Rudnick, Phys. Rev. Lett. **46**, 933 (1981).
[3]G. Meyer-Kress and H. Haken, J. Stat. Phys. **26**, 149 (1981).
[4]Boris Schraiman, C. Eugene Wayne, and Paul C. Martin, Phys. Rev. Lett. **46**, 935 (1981).
[5]J. P. Crutchfield, J. D. Farmer, and B. A. Huberman, Phys. Rep. **92**, 45 (1982).
[6]J. Perez and Carson Jeffries, Phys. Rev. B. **26**, 3460 (1982).
[7]Kurt Wiesenfeld, J. Stat. Phys. (to be published).
[8]J. Guckenheimer and P. J. Holmes, *Nonlinear Oscillations, Dynamical Systems and Bifurcations of Vector Fields* (Springer, Berlin, 1983).
[9]E. Knobloch and K. A. Wiesenfeld, J. Stat. Phys. **33**, 611 (1983).
[10]See, e.g., N. B. Abraham, in *Proceedings of the Workshop on Fluctuations and Sensitivity in Nonequilibrium Systems,* edited by W. Horsthemke and D. Kondepudi (Springer, Berlin, 1984).
[11]See, e.g., *Hydrodynamic Instabilities and the Transition to Turbulence,* edited by H. L. Swinney and J. P. Gollub (Springer, Berlin, 1981).
[12]D. W. Jordan and P. Smith, *Nonlinear Ordinary Differential Equations* (Oxford, New York, 1977).
[13]P. S. Linsay, Phys. Rev. Lett. **47**, 1349 (1981).
[14]J. Perez and C. Jeffries, Phys. Rev. A **26**, 2117 (1982).
[15]J. Perez and C. Jeffries, Phys. Lett. **92A** 82 (1982).
[16]R. W. Rollins and E. R. Hunt, Phys. Rev. Lett. **49**, 1295 (1982).
[17]J. Testa, J. Perez, and C. Jeffries, Phys. Rev. Lett. **48**, 714 (1982).
[18]S. D. Brorson, D. Dewey, and P. S. Linsay, Phys. Rev. A **28**, 1201 (1983).
[19]C. Jeffries and J. Perez, Phys. Rev. A **27**, 601 (1983).
[20]J. M. Perez, Ph.D thesis, University of California, 1983 [Lawrence Berkeley Laboratory Report No. LBL-16898, 1983 (unpublished)].
[21]E. R. Hunt and R. W. Rollins, Phys. Rev. A **29**, 1000 (1984).
[22]Robert van Buskirk and Carson Jeffries (unpublished).
[23]H. Ikezi, J. S. deGrassie, and T. H. Jensen, Phys. Rev. A **28**, 1207 (1983).
[24]See, e.g., Shyh Wang, *Solid State Electronics* (McGraw-Hill, New York, 1966), p. 313ff.
[25]D. W. Jordan and P. Smith, Ref. 12, p. 187.

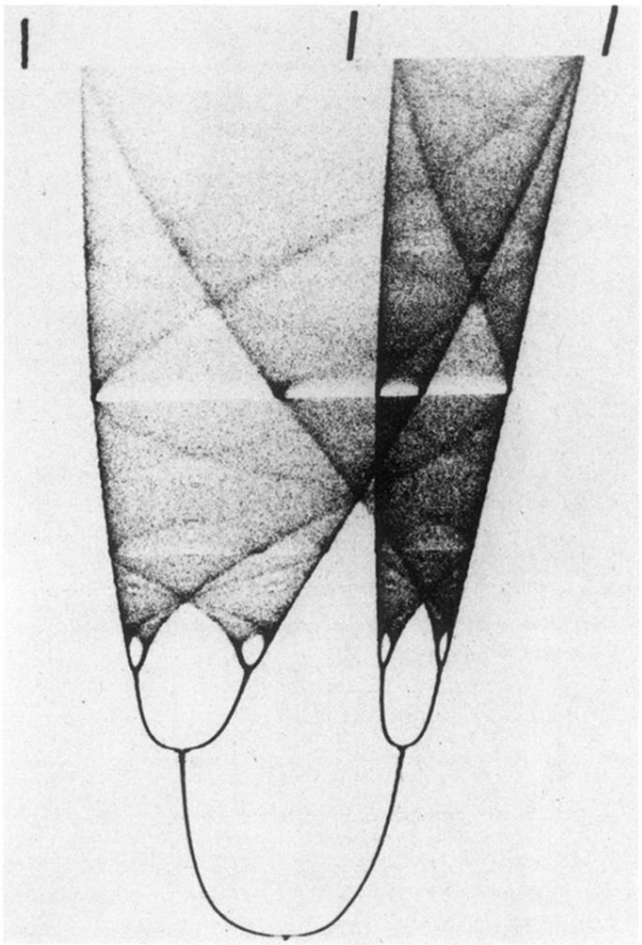

FIG. 3. Typical bifurcation diagram for driven p-n junction (Fig. 2), showing a period doubling cascade, chaos, and periodic windows. Plotted is the set of consecutive current maxima $\{I_n\}$ (horizontal) versus amplitude of sinusoidal drive voltage V_{0S} (vertical).